



Pd(II) and Pt(II) complexes with mixed phosphorus–oxygen donor ligands

Jui-Sui Sun, Calvin E. Uzelmeier, Donald L. Ward and Kim R. Dunbar*

Department of Chemistry, Michigan State University, East Lansing, MI 48824–1322, U.S.A.

(Received 29 September 1997; accepted 31 October 1997)

Abstract A series of new complexes have been synthesized from reactions of $[M(\text{NCCH}_3)_4][\text{BF}_4]_2$ ($M = \text{Pd}, \text{Pt}$) with the mixed donor ligand tris(2,4,6-trimethoxyphenyl) phosphine (TMPP). Reaction of $[\text{Pd}(\text{NCCH}_3)_4][\text{BF}_4]_2$ with two equivalents of TMPP in acetone produces the ether-phosphine complex $[\text{Pd}(\text{TMPP})_2][\text{BF}_4]_2$, **1**. In this molecule the Pd atom is situated at the center of a pseudo-octahedron, with the phosphorus atoms in a *cis* orientation. The complex was also characterized by infrared, electronic, and NMR spectroscopies as well as by cyclic voltammetry. Reaction of $[\text{Pd}(\text{NCCH}_3)_4][\text{BF}_4]_2$ with four equivalents of TMPP in acetone yields the neutral phosphino-phenoxy compound $\text{Pd}(\text{TMPP-O})_2$, **2**, where TMPP-O is the demethylated form of TMPP. ^1H and $^{31}\text{P}\{^1\text{H}\}$ NMR studies of **2** support the assignment of a solution structure that involves free rotation of the uncoordinated phenyl rings of the TMPP ligands. Reaction of $[\text{Pt}(\text{NCCH}_3)_4][\text{BF}_4]_2$ with two equivalents of TMPP in acetonitrile yields $[\text{Pt}(\text{NCCH}_3)_2(\text{TMPP})_2][\text{BF}_4]_2$, **3**. Structural and spectroscopic data for **3** indicate that free rotation of the arene rings in solution is restricted due to steric influences of the two CH_3CN co-ligands. Reaction of $\text{PtCl}_2(\text{NCCH}_3)_2$ with two equivalents of TMPP in acetone or reaction of $[\text{Pt}(\text{NCCH}_3)_4][\text{BF}_4]_2$ with four equivalents of TMPP in acetone gives $\text{Pt}(\text{TMPP-O})_2$, **4**. Reaction of $\text{PtCl}_2(\text{NCCH}_3)_2$ with two equivalents of TMPP in tetrahydrofuran yields the neutral compound $\text{PtCl}(\text{TMPP})(\text{TMPP-O})$, **5**. Although suitable single crystals were not obtained, the structure of compound **5** was deduced from infrared and NMR spectroscopies to be a square planar molecule with one neutral TMPP ligand coordinated in an η^1 fashion and a demethylated TMPP group bound as an $\eta^2\text{-P,O}$ ligand where the phosphorus atoms are *trans* and the other two coordination sites are occupied by a phenoxy oxygen and a Cl atom. © 1998 Elsevier Science Ltd. All rights reserved

Keywords: Pd(II) complex; Pt(II) complex; donor ligands.

Transition metal complexes with ether-functionalized phosphine ligands have been found to exhibit enhanced reactivity due to the presence of weak metal-ether interactions that are often labile in the solid-state as well as in solution [1–4]. As a result of this behavior, ether-phosphine ligands have been referred to as “hemi-labile”, a term coined specifically for such ligands with the complexes themselves being referred to as “incipiently coordinatively unsaturated” [1d,5,6].

In view of the interest in such molecules, our group has been investigating the unusual ether phosphine tris(2,4,6-trimethoxyphenyl)phosphine (TMPP). Special characteristics of this ligand are high basicity, a large cone angle of 184° , and the presence of *ortho*-methoxy substituents that can act as “built-in” solvent

molecules in the chemistry. Among the unusual complexes that have been isolated with this ligand are mononuclear Rh(II) d^7 radicals, molecules that are ordinarily very unstable but which are indefinitely stable towards air and moisture in the presence of TMPP [3a].

One of our goals in this project has been to design homologous series of d^6 , d^7 and d^8 TMPP complexes that differ only in the coordination mode adopted by the TMPP [3]. These related compounds are of general interest for probing the structural and reactivity differences exhibited by compounds that possess the same ligand set but a different metal electron count. Earlier work from our laboratories had shown that homoleptic TMPP compounds of Rh^I, Rh^{II} and Rh^{III} exhibit interesting redox chemistry and that they undergo reversible small molecule reactions based on the ability of the ether groups to dissociate [3a–c,e,n]. Given these promising results, it was logical to extend

* Author to whom correspondence should be addressed.

these studies to Pd(II) and Pt(II) which are known to be useful in catalytic applications when weakly bonded ligands are involved [5j,k,7-9]. In addition, polydentate ligands such as TMPP with steric requirements that favor octahedral coordination may enforce this geometry on metals for which six coordination is rarely observed [10,11]. In spite of the considerable interest, a fairly limited number of such compounds have been studied [5]. During the course of preparing this manuscript, a paper by Lindner and coworkers appeared which describes the reactivity of $[\text{Pd}(\text{P} \cap \text{O})_2]^{2+}$ complexes as CO/ethene copolymerization catalysts, where $\text{P} \cap \text{O}$ is an η^2 -coordinated polysiloxane-bound ether-phosphine [5k]. Herein we report the syntheses, X-ray structures, and spectroscopic data for a series of Pd(II) and Pt(II) complexes supported by TMPP or phenoxide derivatives of TMPP. In the new compounds, the ligands are shown to adopt η^1 , η^2 and η^3 binding modes in square planar or six-coordinate environments. Some of these results have appeared in communication form [3j].

EXPERIMENTAL

Physical measurements

Infrared spectra were recorded on a Nicolet 740 FT-IR spectrophotometer. ^1H NMR spectra were measured on Varian 300 or 500 MHz spectrometers; chemical shifts were referenced relative to the residual proton impurities of acetone- d_6 (2.04 ppm with respect to TMS), acetonitrile- d_3 (1.93 ppm with respect to TMS) or chloroform- d_1 (7.24 ppm with respect to TMS). ^{31}P $\{^1\text{H}\}$ NMR spectra were obtained on Varian 300 or 500 MHz spectrometers operating at 121.4 MHz and 203.6 MHz respectively, and were referenced relative to an external standard of 85% phosphoric acid. Spin-simulation experiments were carried out by using the LAME program which is included in the VNMR software package. Elemental analyses were performed at Galbraith Laboratories, Inc., Knoxville, TN, or Desert Analytics, Tucson, AZ. Electrochemical measurements were carried out by using an EG&G Applied Research Model 362 scanning potentiostat in conjunction with a BAS Model RXY recorder. Cyclic voltammetric experiments were carried out at $22 \pm 2^\circ\text{C}$ using 0.1 M tetra-*n*-butylammonium hexafluorophosphate (TBAPF $_6$) as the supporting electrolyte. $E_{\text{p,a}}$ and $E_{\text{p,c}}$ were referenced to a Ag/AgCl electrode and are uncorrected for junction potentials.

Starting materials

The starting materials $\text{PtCl}_2(\text{NCC}_6\text{H}_5)_2$ and Pd sponge were purchased from Strem Chemicals, Inc. and were used as received. Tris(2,4,6-trimethoxyphenyl)phosphine (TMPP) was prepared according to published methods [3m] or purchased from Aldrich

and used without further purification [12]. $[\text{M}(\text{NCCH}_3)_4][\text{BF}_4]_2$ (M = Pd [13a], Pt [13b]), and $[\text{Cp}_2\text{Fe}][\text{BF}_4]$ [13c] salts were prepared as described in the literature. Acetone was distilled over 3 Å molecular sieves, methanol was distilled over $\text{Mg}(\text{OMe})_2$ under a nitrogen atmosphere, and methylene chloride was distilled over P_2O_5 under a nitrogen atmosphere. Benzene, diethyl ether, THF, and toluene were distilled over sodium-potassium/benzophenone. Unless otherwise specified, all reactions were carried out under an argon atmosphere by using standard Schlenk-line techniques.

$[\text{Pd}(\text{TMPP})_2][\text{BF}_4]_2$ (1). An acetone solution (10 ml) containing two equivalents of TMPP (0.476 g, 0.900 mmol) was added dropwise to an acetone solution (10 ml) of $[\text{Pd}(\text{NCCH}_3)_4][\text{BF}_4]_2$ (0.200 g, 0.450 mmol) at -44°C which effected an immediate color change from pale yellow to red. The resulting solution was stirred for 40 min at -44°C and evaporated to dryness *in vacuo*. The compound was recrystallized from acetone and diethyl ether to give a brick-red solid in 82% yield (0.993 g). ^1H NMR in acetone- d_6 at -80°C (δ ppm): -OMe 3.32 (s, 6H); 3.34 (s, 6H); 3.47 (s, 6H); 3.52 (s, 6H); 3.83 (br, 18H); 4.03 (s, 6H); 4.25 (s, 6H); *meta*-H: 5.70 (br, 2H), 5.92 (br, 2H), 6.19 (br, 2H), 6.30 (br, 2H), 6.43 (br, 2H), 6.78 (br, 2H). $^{31}\text{P}\{^1\text{H}\}$ NMR in acetone- d_6 (300 MHz, δ ppm): +1.67. Anal. Calcd for 1, $\text{PdP}_2\text{C}_{34}\text{O}_{18}\text{H}_{66}\text{B}_2\text{F}_8$: C, 48.22; H, 4.95. Found: C, 48.29; H, 5.05. UV-Vis (CH_2Cl_2): λ_{max} (nm) (ϵ in $\text{M}^{-1}\text{cm}^{-1}$) 485 (2.3×10^4), 373 (3.7×10^4), 260 (1.7×10^5).

$[\text{Pd}(\text{TMPP-O})_2]$ (2). An acetone solution (15 ml) containing four equivalents of TMPP (0.719 g, 1.352 mmol) was added dropwise to an acetone solution (10 ml) of $[\text{Pd}(\text{NCCH}_3)_4][\text{BF}_4]_2$ (0.150 g, 0.338 mmol) at 0°C which effected an immediate color change from pale yellow to orange. The resulting solution was stirred for 2 h at 0°C , then warmed to room temperature and stirred for an additional 12 h. The solvent was removed by evaporation to yield an orange solid. This solid was recrystallized from THF and diethyl ether, then washed with a mixture of hexanes and acetone (v/v 2/3) to remove trace amounts of $[\text{CH}_3\text{-TMPP}][\text{BF}_4]$. The orange product is obtained in 78% yield (0.301 g). ^1H NMR (δ ppm in CDCl_3): -OMe: 3.10 (s, 6H), 3.12 (s, 24H), 3.66 (s, 6H), 3.75 (s, 12H); *meta*-H: 5.34 (br, 2H), 5.80 (br, 8H), 6.13 (br, 2H). $^{31}\text{P}\{^1\text{H}\}$ NMR (300 MHz, δ ppm in CDCl_3), -3.07.

$[\text{Pt}(\text{NCCH}_3)_2(\text{TMPP})_2][\text{BF}_4]_2$ (3). A solution of CH_3CN (10 ml) and two equivalents of TMPP (0.240 g, 0.450 mmol) was added dropwise to 5 ml of a CH_3CN solution of $[\text{Pt}(\text{NCCH}_3)_4][\text{BF}_4]_2$ (0.120 g, 0.225 mmol) at 0°C . The resulting solution was stirred for 40 min at 0°C and the solvent was removed *in vacuo* to give a pale yellow solid. The solid was recrystallized from CH_2Cl_2 and Et_2O ; 73% yield (0.250 g). ^1H NMR (δ ppm in CD_3CN): 3.33 (s, 6H, CH_3CN); -OMe: 3.42 (br, 12H), 3.61 (br, 24H), 3.78 (s, 6H), 4.82 (s, 12H); *meta*-H: 6.11 (t, 4H), 6.15 (d, 8H). $^{31}\text{P}\{^1\text{H}\}$

NMR (300 MHz, δ ppm in CD_3CN), -44.5 (d, $^1J_{\text{PtP}} = 2422$ Hz).

Pt(TMPP-*O*)₂ (4). An acetone solution (20 ml) containing four equivalents of TMPP (0.600 g, 1.13 mmol) was added dropwise to an acetone solution (10 ml) of $[\text{Pt}(\text{NCCCH}_3)_4][\text{BF}_4]_2$ (0.150 g, 0.281 mmol) at 0°C . The resulting solution was stirred for 12 h after which time the solvent was removed by evaporation to give a pale yellow residue. The solid was recrystallized from THF and Et_2O to give a pale yellow solid, which was dissolved in a mixture of THF and Et_2O and filtered through Celite to remove the insoluble methylphosphonium salt, $[\text{CH}_3\text{-TMPP}][\text{BF}_4]$. The volume of the filtrate was reduced under vacuum and the resulting yellow product was washed with Et_2O and dried *in vacuo*. 58% yield (0.201 g). X-ray quality single crystals of $\text{Pt}(\text{TMPP-}O)_2$ were obtained from a solution of the compound in EtCN and Et_2O at 0°C . ^1H NMR (δ ppm in CD_3CN), $-\text{OMe}$: 3.40 (s, 6H), 3.58 (s, 24H), 3.69 (s, 6H), 3.82 (s, 12H); *meta*-H: 5.58 (d-d, 2H), 5.81 (d-d, 2H), 6.15 (d, 8H). $^{31}\text{P}\{^1\text{H}\}$ NMR (300 MHz, δ ppm in CD_3CN), -24.9 (d, $^1J_{\text{PtP}} = 1950$ Hz). Anal. Calcd for $\text{PtP}_2\text{C}_{54}\text{O}_{18}\text{H}_{66}\text{B}_2\text{F}_8$: C, 50.61; H, 4.90. Found: C, 49.57; H, 5.05.

PtCl(TMPP)(TMPP-*O*) (5). A mixture of $\text{PtCl}_2(\text{NCC}_6\text{H}_5)_2$ (0.150 g, 0.318 mmol) and TMPP (0.33 g, 0.636 mmol) were loaded in a Schlenk flask, dissolved in 30 ml of THF and stirred for 2 days under reduced pressure to remove the CH_3Cl (g) by-product. A pale yellow precipitate and a yellow solution were obtained. The precipitate was discarded, the yellow solution was filtered into a second flask, and the volume of the filtrate was reduced under vacuum. Et_2O was then added to precipitate a pale yellow solid, which was washed with a mixture of acetone and Et_2O to remove trace quantities of $[\text{CH}_3\text{-TMPP}]^+$, washed with Et_2O and finally dried under vacuum to yield a pale yellow compound in 40% yield (0.163 g). IR (Nujol, cm^{-1}) $\nu(\text{Pt-Cl})$ 326. ^1H NMR (δ ppm in CD_3CN), $-\text{OMe}$: 3.28 (s, 3H), 3.38 (s, 30H), 3.58 (s, 3H), 3.75 (s, 9H), 3.77 (br, 6H); *meta*-H: 5.29 (m, 1H), 5.38 (m, 1H), 5.99 (d, 6H), 6.04 (d, 4H). $^{31}\text{P}\{^1\text{H}\}$ NMR (500 MHz, δ ppm in CD_3CN), -20.47 (dd, $^1J_{\text{PtP}} = 3212$ Hz, $^2J_{\text{PP}} = 561$ Hz), -26.85 (dd, $^1J_{\text{PtP}} = 2993$ Hz, $^2J_{\text{PP}} = 561$ Hz).

X-ray crystallographic studies

Crystallographic data for compounds **1–4** were collected on a Rigaku AFC6S diffractometer equipped with monochromated Mo-K_α radiation produced by a 2 kW sealed tube generator. Crystallographic computing for **1**, **3**, and **4** was performed on a VAXSTATION 4000 by using the Texsan crystallographic software package [14]. Computing for **2** was performed on a Silicon Graphics Indigo II workstation using the Texsan and SHELXTL [15] software system. Crystal parameters and basic information pertaining

to data collection and structure refinement are summarized in Table 1.

[Pd(TMPP)₂][BF₄]₂ (1). Single crystals of **1** were grown by slow diffusion of diethyl ether into a CH_2Cl_2 solution of compound **1**. A red crystal of dimensions $0.50 \times 0.40 \times 0.36$ mm was secured on the tip of a glass fiber with Dow Corning silicone grease and placed in a cold N_2 (g) stream. Least-squares refinement using 21 well-centered reflections in the range $25 \leq 2\theta \leq 35^\circ$ indicated an orthorhombic crystal system. The data were collected at $-110 \pm 1^\circ\text{C}$ using the ω - 2θ scan technique to a maximum 2θ value of 47° . A total of 4837 reflections was collected, of which 4181 data with $I > 0.01\sigma(I)$ were used for F^2 refinement, and 3298 data with $I > 3.00\sigma(I)$ were used for F refinement. An empirical absorption correction based on azimuthal scans of three reflections near $\chi = 90^\circ$ was applied which resulted in transmission factors ranging from 0.92 to 1.00. The data were corrected for Lorentz and polarization effects. The space group was determined to be $Pna2_1$ based on the observed systematic absences. The structure was solved by the MITHRIL [16] program, and subsequent cycles of DIRDIF [17] were used to locate the atom positions for full-matrix least-squares refinement. The phenyl rings of the TMPP ligands were refined isotropically for the F^2 refinement and treated as rigid groups for the F refinement to reduce the number of parameters. F^2 refinement of 585 parameters resulted in residuals of $R = 0.075$ and $R_w = 0.101$, while refinement on F of 433 parameters resulted in residuals of $R = 0.057$ and $R_w = 0.074$. Attempts to solve the structure in the higher symmetry space group $Pnma$ (#62) were unsuccessful. Both enantiomorphs of the non-centrosymmetric space group $Pna2_1$ (#33) were refined, but no statistically significant difference in the residuals R and R_w (0.0751, 0.1009 for #62 and 0.0750, 0.1009 for #33) were observed.

Pd(TMPP-*O*)₂ · 3.73CH₂Cl₂ · H₂O (2) · 3.73CH₂Cl₂ · H₂O. Single crystals of **2** were grown by a slow diffusion of diethyl ether into a CH_2Cl_2 solution of compound **2**. An orange crystal of dimensions $0.98 \times 0.40 \times 0.22$ mm was secured on the tip of a glass fiber with Dow Corning silicone grease and placed in a cold N_2 (g) stream. Least-squares refinement using 25 well-centered reflections in the range $15.0 \leq 2\theta \leq 22.3^\circ$ indicated that the crystal is consistent with an orthorhombic crystal system. The data were collected at $-85 \pm 1^\circ\text{C}$ using the ω - 2θ scan technique to a maximum 2θ value of 47° . Of the 10,169 reflections that were collected, 815 were systematically absent. An empirical absorption correction based on azimuthal scans of three reflections with χ near 90° was applied which resulted in transmission factors ranging from 0.55–1.00. The data were corrected for Lorentz and polarization effects. The structure was solved in the space group $Pbcn$ using the MITHRIL [16] and DIRDIF [17] structure solution programs and refined by full-matrix least-squares refinement on F [15]. Methoxy methyl groups centered about atoms

Table 1. Summary of crystallographic data for [Pd(TMPP)₂][BF₄]₂ (1), Pd(TMPP-*O*)₂ (2) · 3.73CH₂Cl₂ · H₂O, [Pt(NCCH₃)₂(TMPP)₂][BF₄]₂ (3), Pt(TMPP-*O*)₂ (4) · 3EtCN

| | 1 | 2 · 3.73CH ₂ Cl ₂ · H ₂ O | 3 | 4 · 3EtCN |
|--|--|--|---|---|
| Formula | PdP ₂ F ₈ O ₁₈ C ₅₈ B ₂ H ₆₆ | PdCl _{7.5} P ₂ O ₁₉ C _{55.7} H _{67.5} | PtP ₂ F ₈ O ₁₈ N ₇ C ₅₈ BH ₇₂ | PtP ₂ O ₁₈ N ₃ C ₆₁ H ₇₅ |
| Formula weight | 1345.07 | 1376.27 | 1515.85 | 1395.31 |
| Color | Red | Orange | Yellow | Yellow |
| Crystal size (mm ³) | 0.36 × 0.40 × 0.50 | 0.22 × 0.40 × 0.98 | 0.30 × 0.30 × 0.44 | 0.27 × 0.36 × 0.36 |
| Space group | <i>Pna</i> 2 ₁ | <i>Pbcn</i> | <i>P</i> ₋₁ | <i>P</i> 2 ₁ / <i>c</i> |
| <i>a</i> (Å) | 20.71(1) | 20.162(9) | 14.578(3) | 12.958(5) |
| <i>b</i> (Å) | 17.838(3) | 24.62(2) | 18.291(3) | 33.262(7) |
| <i>c</i> (Å) | 15.908(2) | 24.326(11) | 13.229(2) | 14.697(5) |
| α (°) | 90 | 90 | 104.40(1) | 90 |
| β (°) | 90 | 90 | 109.24(1) | 100.68(3) |
| γ (°) | 90 | 90 | 88.41(2) | 90 |
| <i>V</i> (Å ³) | 5876(5) | 12,566(11) | 3220(1) | 6225(3) |
| <i>Z</i> | 4 | 8 | 2 | 4 |
| <i>d</i> _{calc} (g cm ⁻³) | 1.520 | 1.455 | 1.563 | 1.489 |
| <i>m</i> (cm ⁻¹) | 4.56 | 6.47 | 23.38 | 23.96 |
| Temperature (°C) | -110 ± 1 | -85 ± 1 | -100 ± 1 | -100 ± 1 |
| <i>R</i> ^a | 0.075 | 0.1065 | 0.036 | 0.042 |
| <i>R</i> _w ^b , <i>wR</i> ₂ ^c | 0.101 ^b | 0.2598 ^c | 0.045 ^b | 0.047 ^b |
| Goodness of Fit ^d | 2.28 | 1.030 | 1.64 | 1.39 |

$$^a R = \Sigma ||F_o| - |F_c|| / \Sigma |F_o|.$$

$$^b R_w = [\Sigma w(|F_o| - |F_c|)^2 / \Sigma w|F_o|^2]^{1/2}; w = 1/s^2(|F_o|).$$

$$^c wR_2 = [S[w(F_o^2 - F_c^2)^2] / S[w(F_o^2)^2]]^{1/2}.$$

$$^d \text{Goodness-of-fit} = [S w(|F_o| - |F_c|)^2 / (N_{\text{obs}} - N_{\text{parameter}})]^{1/2}.$$

C39, C47, and C48 were found to be disordered, and each was refined isotropically as twin methyl groups, A and B, with a combined occupancy of 1.0 and with restraints on C—O and C...C. All other non-hydrogen atoms were refined anisotropically, except for solvent molecules. Treatment of the dichloromethane molecules is described in the following section. The final full-matrix least-squares refinement was based on 9199 reflections that were used to fit 774 parameters with 540 restraints to give $R_1 = 0.1065$ and $wR_2 = 0.2598$. The goodness-of-fit index was 1.030, and the maximum shift in the final difference map was 0.002 Å³ associated with C173. After convergence, the mean shift/ESD was 0.006 and the highest peak in the difference Fourier map was 1.16 e Å⁻³ which is associated with the solvent molecule containing C172.

Dichloromethane molecules were located using electron density difference maps generated using the SHELXTL software package [15]. The disordered CH₂Cl₂ molecules were modeled with restraints on the C—Cl and C...Cl distances. All C—Cl bond distances were constrained to 1.79 Å. Occupancies were also refined, resulting in a total of 3.73 dichloromethane molecules per Pd atom. An additional isolated atom was added as the oxygen of a water molecule and refined isotropically.

[Pt(NCCH₃)₂(TMPP)₂][BF₄]₂ (3). Single crystals of 3 were grown by slow diffusion of diethyl ether into a solution of 3 in acetone and CH₂Cl₂. A pale yellow crystal of dimensions 0.30 × 0.44 × 0.30 mm³ was

secured on the tip of a glass fiber with Dow Corning silicone grease and placed in a cold N₂(g) stream. Least-squares refinement using 21 well-centered reflections in the range 20 ≤ 2θ ≤ 26° indicated a triclinic crystal system. The data were collected at -100 ± 1°C using the ω-2θ scan technique to a maximum 2θ value of 47°. Of the 9951 reflections that were collected, 9519 were unique. An empirical absorption correction based on azimuthal scans of three reflections with χ near 90° was applied which resulted in transmission factors ranging from 0.84 to 1.00. The data were corrected for Lorentz and polarization effects. The structure was solved in the space group *P* $\bar{1}$ with the program PHASE [18] followed by DIRDIF [17] structure solution programs and refined by full-matrix least-squares refinement. All non-hydrogen atoms were refined anisotropically. The final full-matrix least-squares refinement was based on 7081 observed reflections with $F_o^2 > 3\sigma(F_o^2)$ that were used to fit 820 parameters to give $R = 0.036$ and $R_w = 0.045$. The goodness-of-fit index was 1.64, and the highest peak in the final difference map was 1.59 e Å⁻³ which is associated with the [BF₄]⁻ counterion.

Pt(TMPP-*O*)₂ · 3EtCN (4) · 3EtCN. A pale yellow crystal of dimensions 0.36 × 0.36 × 0.27 mm³ was secured on the tip of a glass fiber with Dow Corning silicone grease and placed in a cold N₂(g) stream. Least-squares refinement using 21 well-centered reflections in the range 20 ≤ 2θ ≤ 24° indicated that the crystal belonged to a monoclinic crystal system.

The data were collected at $-100 \pm 1^\circ\text{C}$ using the ω -scan technique to a maximum 2θ value of 47° . Of the 9900 reflections that were collected, 9420 were unique and were corrected for Lorentz and polarization effects. The space group was determined to be $P2_1/c$ based on the observed systematic absences. An empirical absorption correction based on azimuthal scans of three reflections with χ near 90° was applied which resulted in transmission factors ranging from 0.95 to 1.00. The structure was solved and developed with the use of the MITHRIL [16] and DIRDIF [17] structure solution programs and refined by full-matrix least-squares refinement. All non-hydrogen atoms were refined anisotropically, with the final cycle being based on 6082 observed reflections with $F_o^2 > 3\sigma(F_o^2)$ that were used to fit 766 parameters to give $R = 0.042$ and $R_w = 0.047$. The goodness-of-fit index was 1.39 and the highest peak in the final difference map was $0.85 \text{ e } \text{\AA}^{-3}$.

RESULTS AND DISCUSSION

Preparation of Pd^{II} TMPP complexes

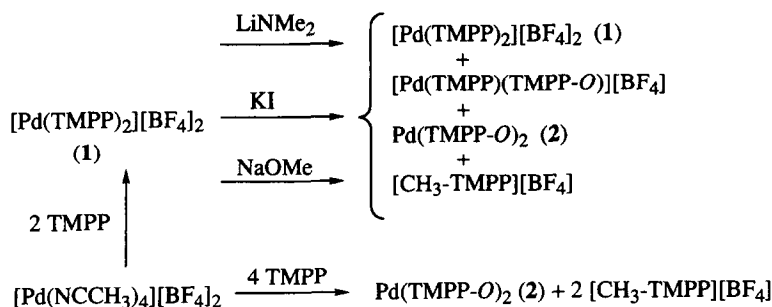
The unusual brick-red compound $[\text{Pd}(\text{TMPP})_2][\text{BF}_4]_2$ (**1**) is readily prepared from $[\text{Pd}(\text{NCCH}_3)_4][\text{BF}_4]_2$ and two equivalents of TMPP in acetone. This compound is thermally unstable in solution, however, and readily converts to the phenoxide derivative $\text{Pd}(\text{TMPP-O})_2$ (**2**) where TMPP-O refers to the monodemethylated derivative of TMPP. The demethylation reaction is accelerated in the presence of excess TMPP which acts as a nucleophile to react with the electrophilic methoxy groups associated with the metal. This type of decomposition reaction has been previously documented in the analogous Rh, Co and Ni compounds [3b,g,i,l], as well as in the chemistry of TMPP with Rh and Ir olefins [3k]. In an effort to avoid sacrificing TMPP in a rational synthesis of $\text{Pd}(\text{TMPP-O})_2$, $[\text{Pd}(\text{TMPP})_2][\text{BF}_4]_2$ was combined with other

nucleophiles such as KI, LiNMe_2 , and NaOMe. Unfortunately, these reactions led to complex mixtures of $[\text{CH}_3\text{-TMPP}][\text{BF}_4]$, **1** and **2**, as evidenced by ^1H and $^{31}\text{P}\{^1\text{H}\}$ NMR spectroscopies. Ultimately, compound **2** was obtained in the best yield and in the purest form from the reaction of $[\text{Pd}(\text{NCCH}_3)_4][\text{BF}_4]_2$ with four equivalents of TMPP (75% yield). The reaction of Pd(II) with TMPP are summarized in Scheme 1.

Preparation of Pt^{II} TMPP complexes

The compound $[\text{Pt}(\text{TMPP})_2][\text{BF}_4]_2$ is obtained from acetone solutions of $[\text{Pt}(\text{NCCH}_3)_4][\text{BF}_4]_2$ that have been treated with two equivalents of TMPP. The product of the same reaction performed in CH_3CN is $[\text{Pt}(\text{NCCH}_3)_2(\text{TMPP})_2][\text{BF}_4]_2$ (**3**) as verified by X-ray crystallography. In $[\text{Pt}(\text{NCCH}_3)_2(\text{TMPP})_2][\text{BF}_4]_2$ only two of the original CH_3CN ligands have been replaced with monodentate TMPP molecules; obviously the ether interactions are prevented due to the presence of the more basic CH_3CN ligands.

$\text{PtCl}_2(\text{NCC}_6\text{H}_5)_2$ was found to react with TMPP in the presence of two equivalents of NaBPh_4 to yield $\text{Pt}(\text{TMPP-O})_2$ (**4**), $\text{PtCl}(\text{TMPP})(\text{TMPP-O})$ (**5**), NaCl, and $[\text{CH}_3\text{-TMPP}][\text{BPh}_4]$. These reactions are designed to make use of the chloride ligands for dealkylation of the *ortho*-substituted methoxy-phosphines with the liberation of MeX [1a,b,d,f]. Single crystals of $\text{Pt}(\text{TMPP-O})_2$ (**4**) were obtained by chilling a $\text{CH}_3\text{CH}_2\text{CN}/\text{Et}_2\text{O}$ solution of the products to 0°C . The presence of **5** suggests that the second *O*-metalation at the remaining chloride ligand is slow and that more forcing conditions are required to drive the reaction to completion. A similar observation was reported by Shaw and co-workers [1a,b,f]. A much higher yield route to $\text{Pt}(\text{TMPP-O})_2$ is the slow addition of an acetone solution of four equivalents of TMPP to an acetone solution of $[\text{Pt}(\text{NCCH}_3)_4][\text{BF}_4]_2$. The reactions of Pt(II) with TMPP are summarized in Scheme 2.

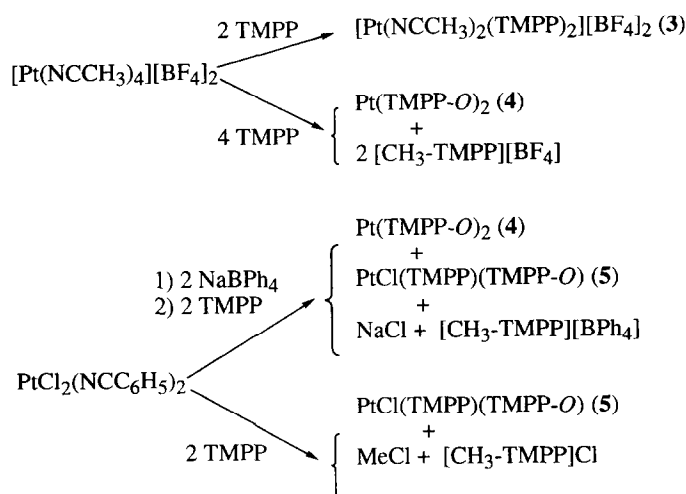


TMPP = $\text{P}\{\text{C}_6\text{H}_2(\text{OCH}_3)_3\}_3$ tris(2,4,6-trimethoxy)phenylphosphine

TMPP-O = $[\text{P}\{\text{OC}_6\text{H}_2(\text{OCH}_3)_2\}\{\text{C}_6\text{H}_2(\text{OCH}_3)_3\}_2]^-$

bis(2,4,6-trimethoxy)phenyl 4,6-trimethoxy-2-phenoxide phosphine

Scheme 1. Reactions of Pd(II) with various nucleophiles.



Scheme 2. Reactions of Pt(II) starting materials with TMPP.

Molecular structures of 1 and 2.

ORTEP drawings of the molecular cation of **1** and **2** are displayed in Figs 1 and 2, with selected bond distances and angles provided in Tables 2 and 3. The Pd atom of **1** resides at the center of a pseudo-octahedron defined by P1, P2 and the two ether-oxygen atoms O1 and O10 in an equatorial arrangement; two ether oxygen atoms O4 and O13 occupy axial

positions. The deviation of the geometry around the Pd atom from square-planar is evident from the acute angles defined by the five-membered metallacycles Pd1—P1—C1—C2—O1 for which P1—Pd1—O1 = 78.3(2)° and Pd1—P2—C19—C20—O10 for which P2—Pd1—P10 = 78.1(2)°. The average Pd—O_{axial} distance of 2.651 Å is the shortest axial contact reported to data for a Pd(II) compound [19–22]. In comparison, the corresponding distances in Pd^{II}L₆

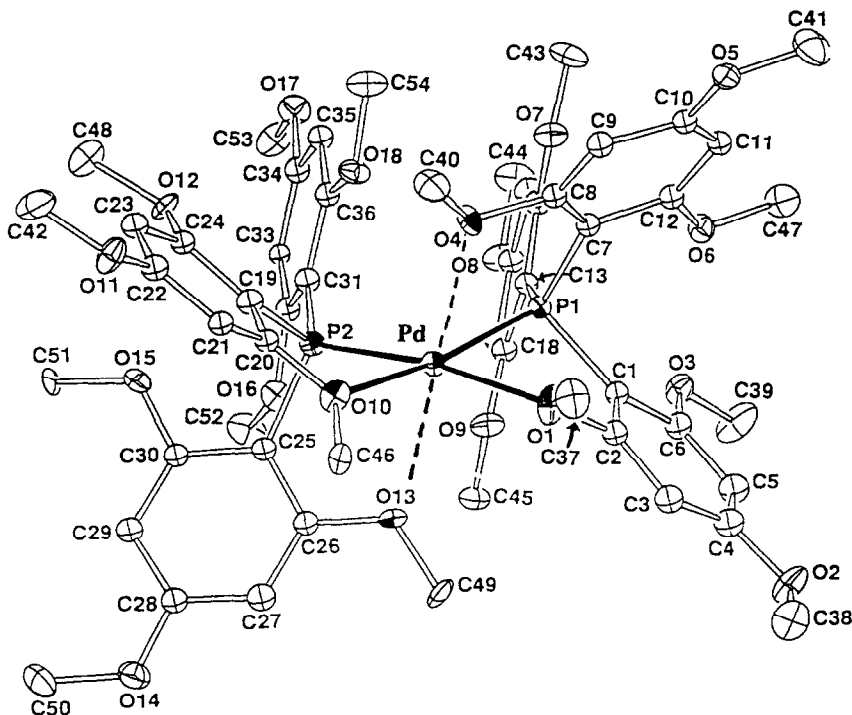


Fig. 1. ORTEP drawing of $[\text{Pd(TMPP)}_2][\text{BF}_4]_2$ (**1**). Thermal ellipsoids are drawn at the 25% probability level. Hydrogen atoms have been removed for clarity. Selected distances (Å) and angles (°) for **1** can be found in Table 3.

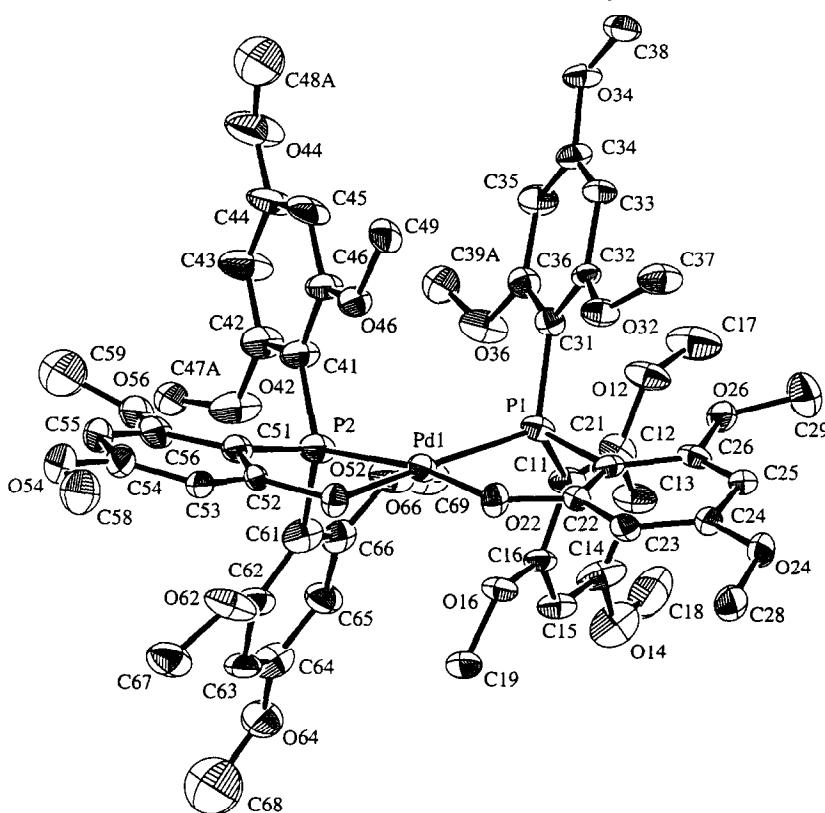


Fig. 2. ORTEP drawing of Pd(TMPP-O)₂ (2). Thermal ellipsoids are drawn at the 25% probability level. Hydrogen atoms have been removed for clarity. Selected distances (Å) and angles (°) for 2 can be found in Table 2.

Table 2. Selected bond distances (Å) and bond angles (°) for [Pd(TMPP)₂][BF₄]₂ (1)

| Bond distances | |
|----------------|-----------|
| Pd1—P1 | 2.216(4) |
| Pd1—P2 | 2.215(4) |
| Pd1—O1 | 2.195(7) |
| Pd1—O10 | 2.177(8) |
| Pd1—O4 | 2.671(7) |
| Pd1—O13 | 2.632(7) |
| P1—C1 | 1.85(1) |
| P1—C7 | 1.82(1) |
| P1—C13 | 1.82(1) |
| P2—C19 | 1.83(1) |
| P2—C25 | 1.82(1) |
| P2—C31 | 1.80(1) |
| Bond angles | |
| P1—Pd1—P2 | 105.92(8) |
| P1—Pd1—O1 | 78.3(2) |
| P1—Pd1—O10 | 168.6(2) |
| P2—Pd1—O1 | 170.1(2) |
| P2—Pd1—O10 | 78.1(2) |
| Pd1—P1—C1 | 96.6(4) |
| Pd1—P1—C7 | 106.1(4) |
| Pd1—P1—C13 | 123.0(4) |
| Pd1—P2—C19 | 96.5(4) |
| Pd1—P2—C25 | 105.7(4) |
| Pd1—P2—C31 | 123.0(4) |

Table 3. Selected bond distances (Å) and bond angles (°) for Pd(TMPP-O)₂ · 3.73CH₂Cl₂O (2 · 3.73CH₂Cl₂ · H₂O)

| Bond distances | |
|----------------|-----------|
| Pd1—P1 | 2.270(4) |
| Pd1—P2 | 2.251(4) |
| Pd1—O22 | 2.047(7) |
| Pd1—O52 | 2.047(8) |
| O22—C22 | 1.363(4) |
| O52—C52 | 1.363(4) |
| P1—C11 | 1.822(13) |
| P1—C21 | 1.832(12) |
| P1—C31 | 1.824(13) |
| P2—C41 | 1.81(2) |
| P2—C51 | 1.78(2) |
| P2—C61 | 1.87(2) |
| Bond angles | |
| P2—Pd1—P1 | 109.4(2) |
| O22—Pd1—P1 | 84.9(2) |
| O52—Pd1—P1 | 165.2(2) |
| O22—Pd1—O52 | 81.2(3) |
| C11—P1—Pd1 | 118.1(5) |
| C21—P1—Pd1 | 97.6(4) |
| C11—P1—C31 | 111.5(6) |
| C11—P1—C21 | 104.2(6) |
| C22—O22—Pd1 | 121.1(7) |
| C52—O52—Pd1 | 117.5(8) |

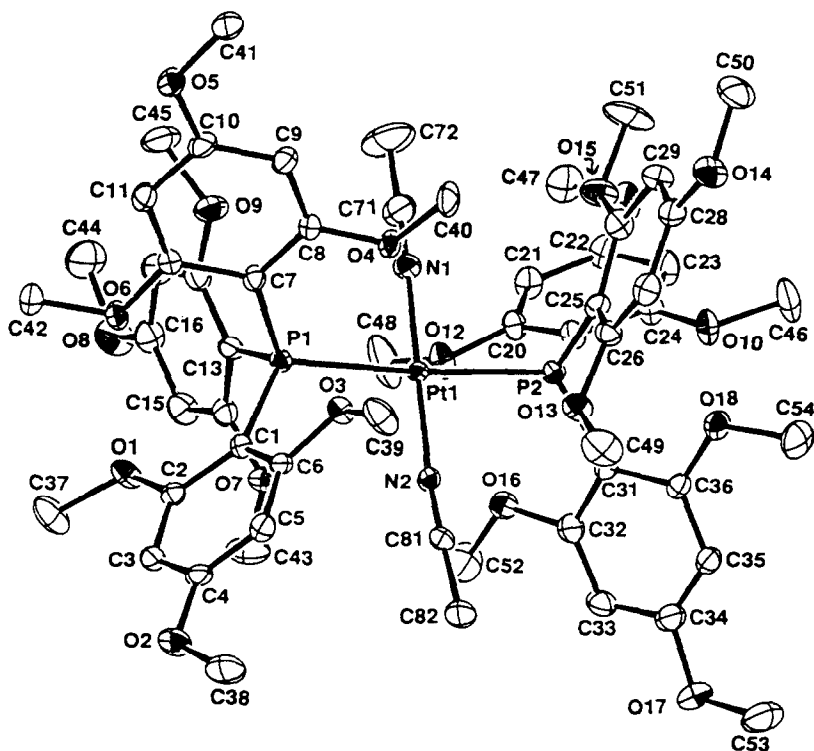
complexes supported by trigonal (*S,S,S*) or (*S,S,N*) ligands fall in the range 2.95–3.27 Å [21–23]. The geometry about the Pd atom of **2** is square planar, consisting of a *cis* arrangement defined by P1, P2 and the phenoxide oxygen atoms O22 and O52. Ring strain in **2** is evidenced by angles of O22—Pd1—O52 = 81.4(3)°, O52—Pd1—P2 = 84.6(2)°, and P2—Pd1—P1 = 109.4(2)°. Axial ether-oxygen atoms O16 and O46 are at distances of 2.887 and 3.025 Å which are much longer than the analogous interactions in **1**.

Molecular structures of **3** and **4**

ORTEP drawings of the compounds [Pt(NCCH₃)₂(TMPP₂)] [BF₄]₂ (**3**) and Pt(TMPP-*O*)₂ (**4**) are presented in Figs 3 and 4, while selected bond distances and angles are provided in Tables 4 and 5, respectively. The coordination number of [Pt(NCCH₃)₂(TMPP₂)] [BF₄]₂ is four with mutually *trans* monodentate TMPP and CH₃CN ligands. The ∠P1—Pt1—N1 and ∠P2—Pt1—N2 angles are 87.0(2)° and 90.3(2)°, respectively, leading to a nearly perfect square planar geometry around the metal center. The *trans* atoms define angles of ∠P1—Pt1—P2 = 175.67(7)° and ∠N1—Pt1—N2 = 177.0(3)°. The molecular geometry of Pt(TMPP-*O*)₂ consists of a *cis* arrangement of phosphorus and methoxy-oxygen atoms about the

metal center and long axial interactions to ether-oxygen atoms. The distortion observed in Pt(TMPP-*O*)₂ involves ring strain of the five-membered metallacycles (Pt1—P1—C1—C2—O1 and Pt1—P2—C19—C20—O10) for which the angles are ∠C2—Pt1—P1 = 84.1(2)° and ∠O10—Pt1—P2 = 84.2(2)° compared to the η¹-TMPP ligands observed in compound [Pt(NCCH₃)₂(TMPP)₂][BF₄]₂ (**3**). Free rotation of arene rings on the η¹-TMPP ligands in **3** is effectively blocked by the CH₃CN ligands, which are in the rotational pathway of pendant methoxy groups of TMPP. This is evident in the space filling diagram of the compound depicted in Fig. 5. The solid-state structure is evidently retained in solution as judged by the results of NMR spectroscopy (*vide infra*).

The average Pt—P bond distances in [Pt(NCCH₃)₂(TMPP₂)] [BF₄]₂ and Pt(TMPP-*O*)₂ of 2.356(2) and 2.255(2) Å respectively are similar to those observed in phosphine and phosphite complexes of Pt(II) (2.2 to 2.4 Å) [23]. The η¹-Pt—P bond distances in [Pt(NCCH₃)₂(TMPP₂)] [BF₄]₂ are longer than those found in Pt(TMPP-*O*)₂ which may be due to the chelate effect of the η²-TMPP ligands in the latter compound and also to the *trans* effect of the TMPP vs the phenoxide ligand. The average Pt—O bond distance of 2.047(5) Å in Pt(TMPP-*O*)₂ is longer than the corresponding bond distance reported in the platinum-alkoxide complex, *cis*-[Pt(PPh₂CH₂CMe₂O)₂]



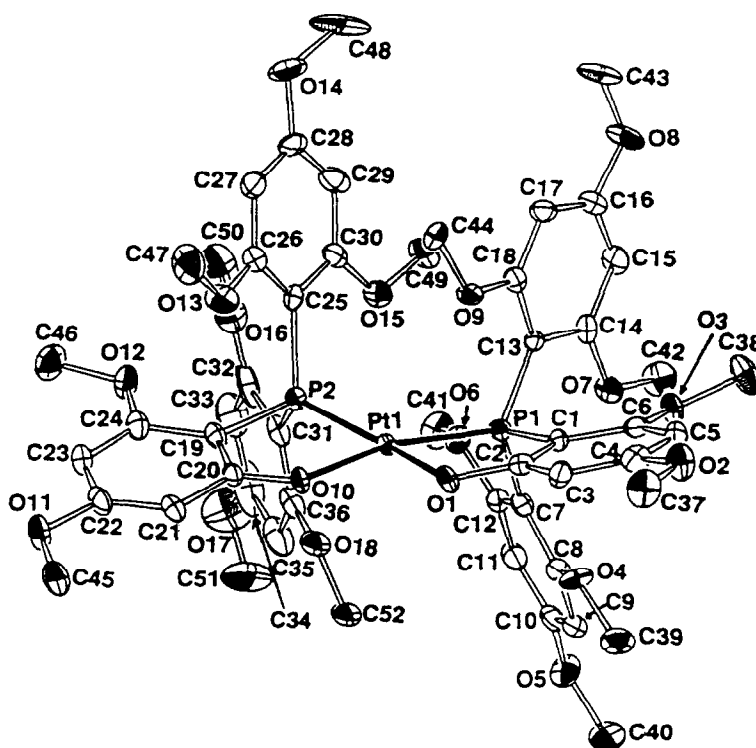


Fig. 4. ORTEP drawing of Pt(TMPP-*O*)₂ (**4**). Hydrogen atoms have been removed for clarity. Thermal ellipsoids are drawn at the 25% probability level. Selected distances (Å) and angles (°) for **4** can be found in Table 5.

(2.013(4) Å) [25a] and *cis*-[Pt(Ph₂PCH₂CH₂O)₂]·H₂O (2.039(5) Å) [25b], but shorter than those found in two platinum-ether complexes (2.144(9) Å and 2.192(7) Å) [5f,g]. Axial interactions in the molecule Pt(TMPP-*O*)₂ that involve the Pt center and pendant

methoxy groups are longer than the sum of the covalent radii of the two atoms (Pt1—O9 = 3.110(5) Å and Pt1—O18 = 3.130(7) Å).

¹H and ³¹P{¹H} NMR studies

Compounds (1) and (2). Variable-temperature ¹H NMR studies of [Pd(TMPP)₂][BF₄]₂ (**1**) in acetone-*d*₆ from +20 to −80°C indicate that the TMPP ligands are involved in a fluxional process which is not unusual for these types of complexes [9]. The ¹H NMR spectrum at 20°C contains a broad resonance at 6.3 ppm due to the *m*-protons of the phenyl rings, a sharp resonance at 3.8 ppm assigned to the equivalent *para*-methoxy substituents and a broad signal at 3.6 ppm due to the *ortho*-methoxy substituents. The ¹H NMR spectrum at −80°C contains three resonances between δ = 3.5–6.5 ppm, six distinct resonances in the range δ = 5.60–6.80 ppm assigned to inequivalent *meta* protons, six resonances between δ = 3.30–4.25 ppm due to inequivalent *ortho*-methoxy groups, and one broad resonance at δ = 3.83 ppm due to three *para*-methoxy substituents. This spectrum is consistent with free rotation of the unmetalated aryl groups. A room temperature ³¹P{¹H} NMR spectrum of **1** in acetone-*d*₆ exhibits a single resonance at δ = +1.67 ppm. These data are in accord with the presence of only one type of coordinated phosphine

Table 4. Selected bond distances (Å) and bond angles (°) for [Pt(NCCH₃)₂(TMPP)₂][BF₄]₂ (**3**)

| Bond distances | | | |
|----------------|-----------|--------|----------|
| Pt1—P1 | 2.357(2) | P1—C1 | 1.822(7) |
| Pt1—P2 | 2.356(2) | P1—C7 | 1.814(7) |
| Pt1—N1 | 1.972(7) | P1—C13 | 1.806(7) |
| Pt1—N2 | 1.961(6) | P2—C19 | 1.810(7) |
| N1—C71 | 1.12(1) | P2—C25 | 1.808(7) |
| N2—C81 | 1.141(9) | P2—C31 | 1.820(7) |
| Bond angles | | | |
| P1—Pt1—P2 | 175.67(7) | | |
| P1—Pt1—N1 | 87.0(2) | | |
| P1—Pt1—N2 | 93.9(2) | | |
| P2—Pt1—N1 | 88.9(2) | | |
| P2—Pt1—N2 | 90.3(2) | | |
| N1—Pt1—N2 | 176.9(3) | | |
| Pt1—N1—C71 | 171.9(8) | | |
| Pt1—N2—C81 | 174.0(6) | | |
| N1—C71—C72 | 176(1) | | |
| N2—C81—C82 | 178.7(8) | | |

Table 5. Selected bond distances (Å) and bond angles (°) for Pt(TMPP-*O*)₂·3EtCN (4·3EtCN)

| Bond distances | | | |
|----------------|-----------|--------|----------|
| Pt1—P1 | 2.255(2) | P1—C1 | 1.810(8) |
| Pt1—P2 | 2.255(2) | P1—C7 | 1.821(9) |
| Pt1—O1 | 2.044(5) | P1—C13 | 1.830(8) |
| Pt1—O10 | 2.049(5) | P2—C19 | 1.817(8) |
| Pt1—O9 | 3.119(5) | P2—C25 | 1.836(9) |
| Pt1—O18 | 3.130(7) | P2—C31 | 1.845(9) |
| Bond Angles | | | |
| P1—Pt1—P2 | 110.85(8) | | |
| P1—Pt1—O1 | 84.1(2) | | |
| P1—Pt1—O10 | 164.0(2) | | |
| P2—Pt1—O1 | 163.2(2) | | |
| P2—Pt1—O10 | 84.2(2) | | |
| Pt1—P1—C1 | 98.7(3) | | |
| Pt1—P1—C7 | 111.9(3) | | |
| Pt1—P1—C13 | 123.5(3) | | |
| Pt1—P2—C19 | 99.1(3) | | |
| Pt1—P2—C25 | 111.0(3) | | |
| Pt1—P2—C31 | 124.0(3) | | |

ligand and support a close relationship between the solution and solid-state structures of the cation. A fluxional process such as this indicates that, for a given phosphine ligand, there are six *ortho*-methoxy oxygen atoms competing for a total of two coordination sites. Such exchange within the coordination sphere is a potentially valuable characteristic for the design of catalytically active complexes.

The ¹H NMR spectrum of Pd(TMPP-*O*)₂ (**2**) reveals only four distinct features in the methoxy

region of the TMPP-*O* ligands between 3.0 and 3.8 ppm, which indicates that the unbound rings on the TMPP ligands are involved in free rotation on the NMR time scale. The Ni(II) analog also behaves in this manner [3i,26]. Two of these four resonances are due to the inequivalent *para* (*a*) and *ortho* (*b*) methyl groups of the bonded ring while the other two are due to four equivalent *ortho* (*c*) and two equivalent *para* (*d*) methyl groups of the free rings, as depicted in Fig. 6. Three distinct resonances appear in the *meta* proton region of TMPP-*O* ligands between 5.3 and 6.2 ppm. Two of these three resonances are assigned to two inequivalent *meta* protons (1 and 2) of the bonded ring and the third one is attributed to four equivalent *meta* protons (3) of the free rings as indicated on the spectrum. A ³¹P{¹H} NMR spectrum of Pd(TMPP-*O*)₂ (**2**) in chloroform-*d*₁ at room temperature exhibits a single resonance at δ = -3.07 ppm.

Compounds 3–5. The room temperature ¹H NMR spectrum of [Pt(NCCH₃)₂(TMPP)₂][BF₄]₂ (**3**) (Fig. 7) reveals six distinct resonances in the methoxy region between 3.3 and 3.9 ppm and two resonances in the *meta* proton region between 6.1 and 6.2 ppm due to the TMPP ligands. This pattern indicates that the solution structure of **3** possesses two magnetically inequivalent methoxyphenyl rings which is consistent with the solid-state structure as mentioned earlier. An assignment of the resonances in [Pt(NCCH₃)₂(TMPP)₂][BF₄]₂ is provided in the inset on the NMR spectrum in Fig. 7. Two rings above and below the plane defined by the three atom sequence P—Pt—P are symmetry related by a mirror plane bisecting the third ring and containing the two phosphorus atoms and the metal center. One singlet at 3.33 ppm is assigned to two CH₃CN ligands (*a*), while the res-

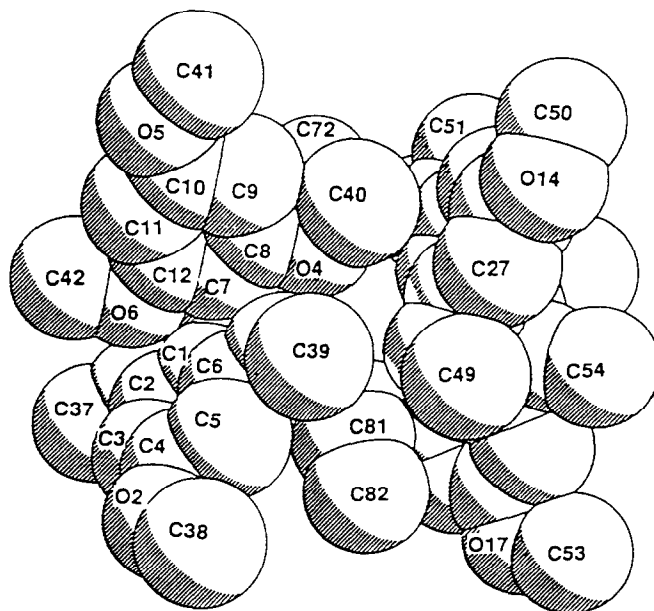


Fig. 5. Space filling diagram of [Pt(NCCH₃)₂(TMPP)₂][BF₄]₂ (**3**). Hydrogen atoms have been removed for clarity.

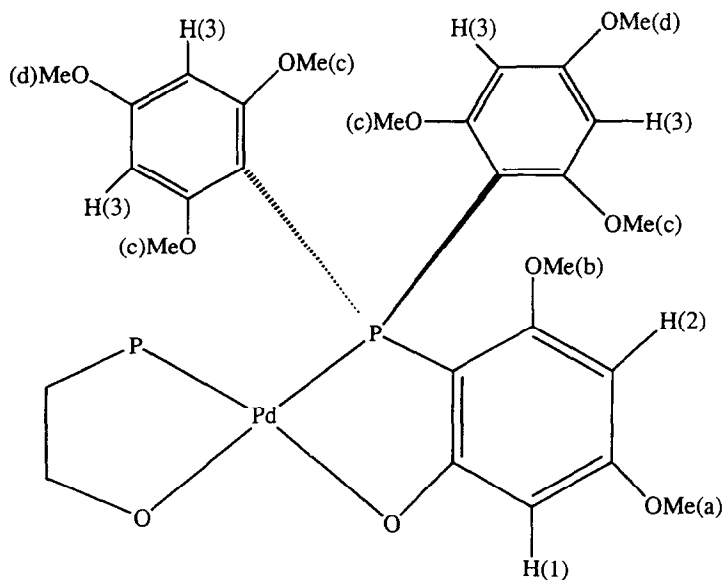


Fig. 6. Illustration of Pd(TMPP-O)₂ (2) with hydrogen atoms labeled. The other half of the molecule is omitted for clarity.

onances at 3.41 and 3.78 ppm are assigned to be the *ortho* (b) and *para* (c) methyl groups on the rings of the TMPP ligands distal from the CH₃CN groups. The two resonances at 3.61 and 3.82 ppm are assigned to the *ortho* (d) and *para* (e) methyl groups on the rings of TMPP ligands proximal to CH₃CN. The triplet and the doublet are attributable to four equivalent *meta* (1) protons on the two distal rings and eight protons (2) on the four proximal phenyl groups rings. The virtual triplet observed in the *meta* proton region of

the TMPP ligand is indicative of a *trans* geometry for the two phosphorus atoms, which is supported by the X-ray structure.

The room temperature ¹H NMR spectrum of Pt(TMPP-O)₂ (4), shown in Fig. 8, resembles that of Pd(TMPP-O)₂ and contains four distinct resonances in the methoxy region of the TMPP-phenoxide ligands between 3.3 and 3.9 ppm. This indicates that the unbound rings of the TMPP ligand are free to rotate which has also been observed in the Ni(II) [3i,26] and

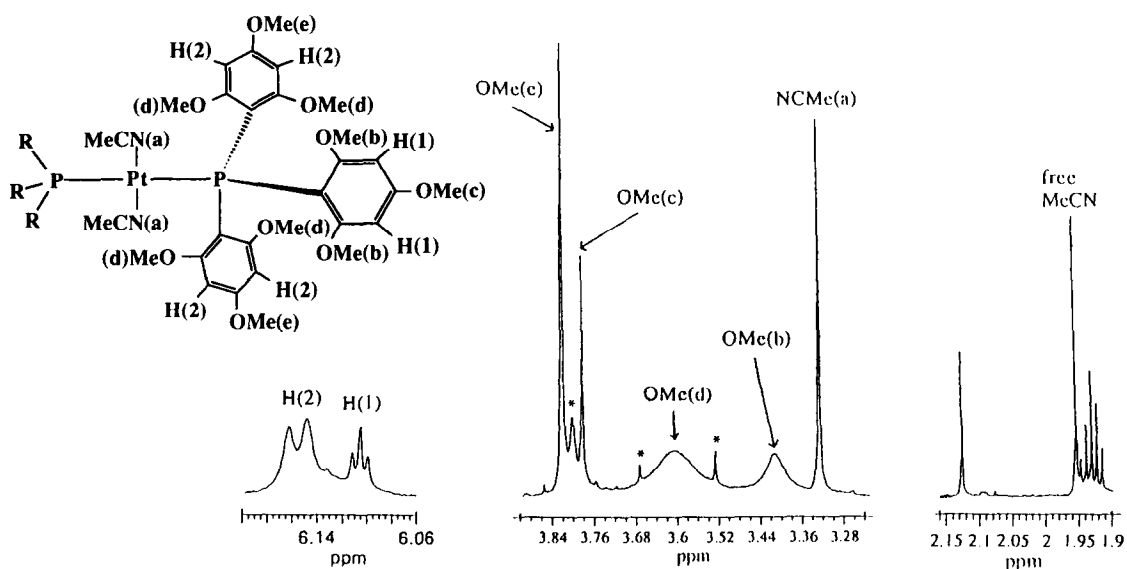


Fig. 7. Room temperature ¹H NMR spectrum of [Pt(NCCH₃)₂(TMPP)₂][BF₄]₂ (3). (*) Signals due to demethylation products that are always present in small quantities.

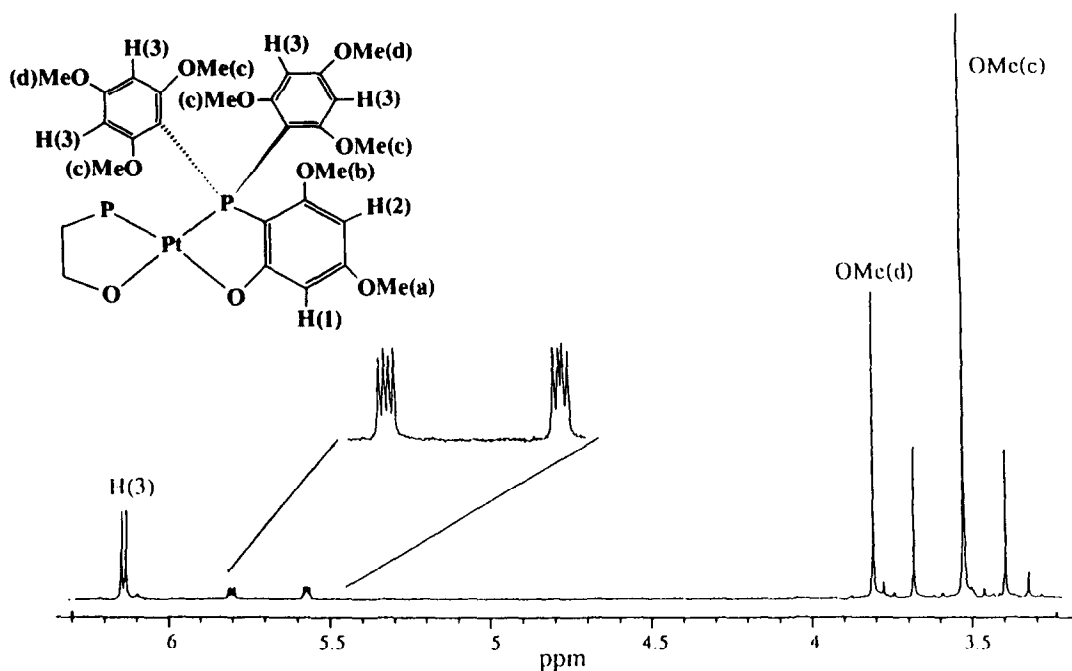


Fig. 8. Room temperature ^1H NMR spectrum of $\text{Pt}(\text{TMPP-}O)_2$ (**4**) in acetonitrile- d_3 .

$\text{Pd}(\text{II})$ analogues [3j]. Two of these four resonances are due to the inequivalent *ortho* and *para* methoxy groups of the bonded ring and the other two are due to four equivalent *ortho* and two equivalent *para* methoxy groups of the free rings. Three distinct resonances occur in the *meta* proton region between 5.5 and 6.2 ppm. Two of these three resonances are due to two inequivalent *meta* protons of the bonded ring and the last one is due to four equivalent *meta* protons of the free rings. A $^{31}\text{P}\{^1\text{H}\}$ NMR spectrum of $\text{Pt}(\text{TMPP-}O)_2$ in acetonitrile- d_3 at room temperature exhibits a single resonance at $\delta = -24.97$ ppm with a coupling constant $^1J_{\text{Pt-P}}$ of 1950 Hz, which is in the range of values reported in the literature for *cis* phosphine ligands [23]. Despite the increased electron density at the metal center in the neutral compound **4**, the ^{31}P spectrum exhibits a downfield shift as compared to $\delta = -44.5$ ppm for the dicationic complex **3**. Such a shift can be explained by ring contributions from the formation of five-membered rings [24]. These NMR data are in accord with the presence of two types of unsymmetrically coordinated rings of the TMPP ligand.

The room temperature ^1H NMR spectrum of $\text{PtCl}(\text{TMPP})(\text{TMPP-}O)$ (**5**) (Fig. 9) reveals five resonances in the methoxy region of the TMPP and TMPP-*O* ligands between 3.2 and 3.9 ppm. These data indicate that the unbound rings of the bidentate TMPP ligand are involved in free rotation. Two of these five resonances are due to the inequivalent *ortho* (a) and *para* (b) methoxy groups of the bonded ring of the TMPP-*O* moiety, while a second set are due to the *para* (c and d) methoxy groups on the free rings

of the TMPP and TMPP-*O* ligands. Integration requires the fifth resonance to be an overlap of *ortho* (e) methoxy groups on the free rings of both the TMPP and TMPP-*O* ligands. Four distinct features in the *meta* proton region of TMPP and TMPP-*O* ligands appear between 5.3 and 6.1 ppm. Two multiplets at 5.29 and 5.38 ppm are due to the two *meta* (H1 and H2) protons of the bonded ring of the TMPP-*O* moiety, while a doublet at 6.04 ppm is attributed to four *meta* (H3) protons of the free rings. The final doublet at 5.99 ppm is assigned to six equivalent *meta* (H4) protons of the η^1 -TMPP ligand. A $^{31}\text{P}\{^1\text{H}\}$ NMR spectrum of **5** in acetonitrile- d_3 at room temperature exhibits an ABX second-order pattern with satellites, indicating the presence of two inequivalent phosphorus atoms coupled to ^{195}Pt ($I = 1/2$, 33% abundance) [1a-c,23]. Successful simulation of this spectrum was obtained by first simulating the ABX splitting pattern which gave the satellite positions, followed by simulation of the AB $\text{P}_A\text{—P}_B$ coupling. These two simulations were then combined with appropriate weighting of the satellite intensities. The best fit was achieved with chemical shift values of P_A , $\delta = -20.48$ ppm, P_B , $\delta = -26.39$ ppm and coupling constants of $^1J(\text{Pt—P}_A) = 3212$ Hz, $^1J(\text{Pt—P}_B) = 2993$ Hz and $^2J(\text{P}_A\text{—P}_B) = 561$ Hz (Fig. 9). These NMR data are in accord with the molecular geometry depicted in Fig. 10 wherein one neutral TMPP ligand is coordinated in an η^1 fashion and a demethylated TMPP group is bound as an η^2 -P,O ligand with *trans* P atoms (deduced from the large magnitude of $^2J(\text{P}_A\text{—P}_B)$), a phenoxide O and a Cl^- ion in a square plane.

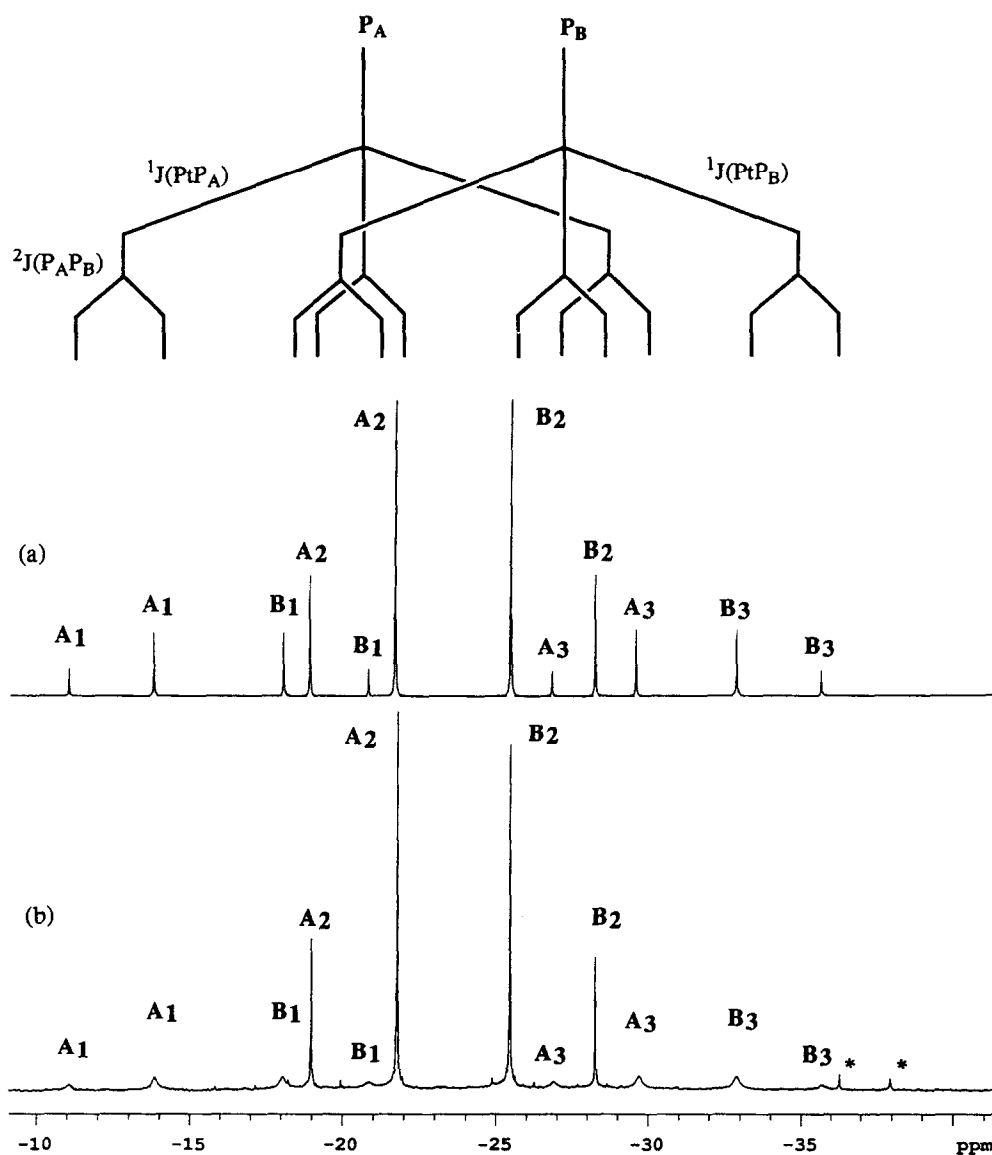


Fig. 9. The splitting diagram for (a), calculated and (b) experimental $^{31}\text{P}\{^1\text{H}\}$ NMR spectrum of $\text{PtCl}(\text{TMPP})(\text{TMPP}-O)$ (5) in acetonitrile- d_3 at room temperature. (*) Signals due to demethylation products that are always present in small quantities.

CONCLUSIONS

Reactions of divalent palladium and platinum complexes with 2,4,6-tris(trimethoxyphenyl)phosphine lead to the formation of new phosphinoether and phosphinophenoxide compounds including a six-coordinate Pd(II) complex possessing the shortest axial contacts reported in the literature to date. Unlike most other P,O chelates reported in the literature, the TMPP ligand appears to be sufficiently flexible to adopt a myriad of bonding modes. This point is well-demonstrated by the observed hapticity changes of TMPP from monodentate in $[\text{Pt}(\text{NCCCH}_3)_2(\text{TMPP})_2][\text{BF}_4]_2$ (3) to bidentate in $\text{Pd}(\text{TMPP}-O)_2$ (2) and

$\text{Pt}(\text{TMPP}-O)_2$ (4) to tridentate in $[\text{Pd}(\text{TMPP})_2][\text{BF}_4]_2$ (1). The results of this study, taken together with the data obtained in earlier investigations, support the conclusion that homoleptic TMPP complexes of the platinum group metals are fairly unstable due to electrophilic reactions of the coordinated methoxy groups that lead to phenoxide formation. It appears that the TMPP phosphine molecule itself is the most useful demethylation reagent for the high-yield preparation of the demethylated compounds $\text{M}(\text{TMPP}-O)_2$ ($\text{M} = \text{Pd}, \text{Pt}$), with other nucleophiles being much less specific in their reactions with $[\text{M}(\text{TMPP})_2]^{2+}$ species. The fluxional nature of $[\text{Pd}(\text{TMPP})_2][\text{BF}_4]_2$ allows for the *in situ* formation of open coordination sites which

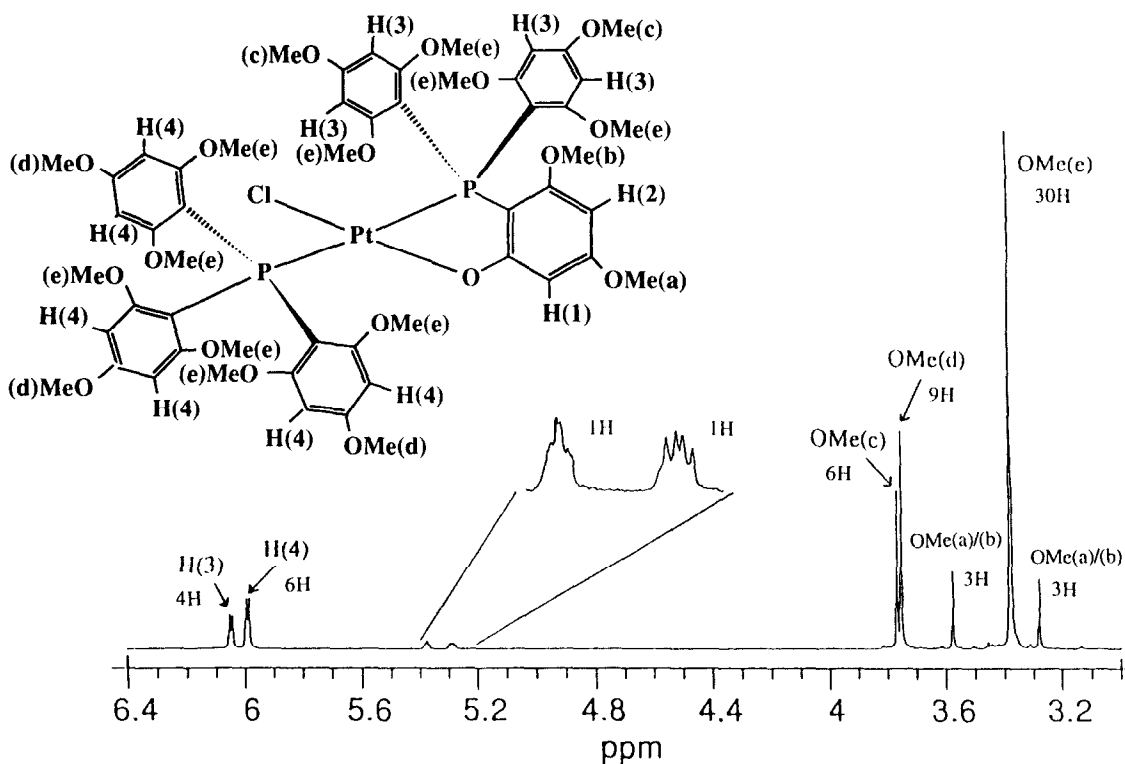


Fig. 10. Room temperature ^1H NMR spectrum of $\text{PtCl}(\text{TMPP})(\text{TMPP-O})$ (**5**) in acetonitrile- d_3 .

opens up the potential for small molecule activation or catalytic activity, possibilities that are currently being explored.

Acknowledgements—We gratefully acknowledge the National Science Foundation (Grant CHE-8914915 to K.R.D.) and the Camille and Henry Dreyfus Foundation for financial support. We also thank Michigan State University for providing The Herbert T. Graham fellowship for C.E.U. The X-ray equipment was purchased by grants from the National Science Foundation (Grants CHE-8403823 and CHE-8908088). The NMR equipment was supported by a grant from the National Institutes of Health (Grant No. 1-510-RR04750-01).

Supporting information available—

Tables of crystal data, atomic coordinates, bond lengths and angles, anisotropic displacement parameters, and positional and thermal parameters for **1**, **2**, **3**, and **4** (51, 70, 75 and 67 pages, respectively). Ordering information is given on any current masthead page.

REFERENCES

- (a) Jones, C. E., Shaw, B. L. and Turtle, B. L., *J. Chem. Soc., Dalton Trans.*, 1974, 992; (b) Empsall, H. D., Shaw, B. L. and Turtle, B. L., *J. Chem. Soc., Dalton Trans.*, 1976, 1500; (c) Empsall, H. D., Heys, P. N. and Shaw, B. L., *J. Chem. Soc., Dalton Trans.*, 1978, 257; (d) Jeffrey, J. C. and Rauchfuss, T. B., *Inorg. Chem.*, 1979, **18**, 2658; (e) Moulton, C. J. and Shaw, B. L., *J. Chem. Soc., Dalton Trans.*, 1980, 299; (f) Miller, E. M. and Shaw, B. L., *J. Chem. Soc., Dalton Trans.*, 1974, 480.
- See for example: Lindner, E. and Dettinger, J. Z., *Naturforsch.*, 1991, **46b**, 432 and references therein.
- (a) Dunbar, K. R., Haefner, S. C. and Pence, L. E., *J. Am. Chem. Soc.*, 1989, **111**, 5504; (b) Dunbar, K. R., Haefner, S. C. and Bender, C., *J. Am. Chem. Soc.*, 1991, **113**, 9540; (c) Dunbar, K. R., Haefner, S. C. and Swepston, P. N., *J. Chem. Soc., Chem. Commun.*, 1991, 460; (d) Chen, S.-J. and Dunbar, K. R., *Inorg. Chem.*, 1991, **30**, 2918; (e) Dunbar, K. R. and Haefner, S. C., *Organometallics*, 1992, **11**, 1431; (f) Dulebohn, J. I., Haefner, S. C., Bergland, K. R. and Dunbar, K. R., *Chem. of Mat.*, 1992, **4**, 506; (g) Dunbar, K. R. and Quilleveré, A., *Organometallics*, 1993, **12**, 618; (h) Dunbar, K. R., Matonic, J. H. and Saharan, V., *Inorg. Chem.*, 1994, **33**, 25; (i) Dunbar, K. R., Quilleveré, A. and Sun, J.-S., *Inorg. Chem.*, 1994, **33**, 3598; (j) Dunbar, K. R. and Sun, J.-S., *J. Chem. Soc., Chem. Comm.*, 1994, 2387; (k) Dunbar, K. R., Haefner, S. C., Uzelmeier, C. E. and Howard, A., *Inorg. Chim. Acta*, 1995, **240**, 527; (l) Quilleveré, A., Sun, J.-S., Uzelmeier, C. E. and Dunbar, K. R., manuscript in preparation; (m) Dunbar, K. R. and Haefner, S. C., *Polyhedron*, 1994, **13**, 727; (n) Haefner, S. C.,

- Uzelmeier, C. E. and Dunbar, K. R., manuscript in preparation.
- Werner, H., Stakr, A., Schultz, M. and Wolf, J., *Organometallics*, 1992, **11**, 1126.
 - (a) Anderson, G. K. and Kumar, R., *Inorg. Chem.*, 1984, **23**, 4064; (b) Braunstein, P., Matt, D. and Dusausay, Y., *Inorg. Chem.*, 1983, **22**, 2043; (c) Podlahová, J., Kratochvil, B. and Langer, V., *Inorg. Chem.*, 1981, **20**, 2160; (d) Empsall, H. D., Johnson, S. and Shaw, B. L., *J. Chem. Soc., Dalton Trans.*, 1980, 302; (e) O'Flynn, K. H. P. and McDonald, W. S., *Acta Cryst.*, 1977, **B33**, 194; (f) Anderson, G. K., Corey, E. R. and Kumar, R., *Inorg. Chem.*, 1987, **26**, 97; (g) Alcock, N. W., Platt, A. W. G. and Pringle, P. G., *J. Chem. Soc., Dalton Trans.*, 1989, 2069; (h) Reddy, V. V. S., Whitten, J. E., Redmill, K. A., Varshney, A. and Gray, G. M., *J. Organomet. Chem.*, 1989, **372**, 207; (i) Braunstein, P., Matt, D., Dusausoy, Y., Fischer, J., Mitschler, A. and Ricard, L., *J. Am. Chem. Soc.*, 1981, **103**, 5115; (j) Lindner, E., Schrieber, R., Kemmler, M., Schneller, T. and Mayer, H. A., *Chem. Mater.*, 1995, **7**, 1951; (k) Lindner, E., Schrieber, R., Schneller, T., Wegner, P. and Mayer, H. A., *Inorg. Chem.*, 1996, **35**, 514.
 - Bader, A. and Lindner, E., *Coord. Chem. Rev.*, 1991, **108**, 27.
 - (a) Peuckert, M. and Keim, W., *Organometallics*, 1983, **2**, 594; (b) Huang, Q., Xu, M., Qian, Y., Xu, W., Shao, M. and Tang, Y., *J. Organomet. Chem.*, 1985, **287**, 419; (c) Keim, W., Behr, A., Hoffmann, B., Kowaldt, F. H., Kürschner, U., Limbäcker, B. and Sistig, F., *Organometallics*, 1986, **5**, 2356; (d) Klabunde, U. and Ittel, S. D., *J. Molec. Catal.*, 1987, **41**, 123.
 - (a) Schrock, R. R. and Osborn, J. A., *J. Am. Chem. Soc.*, 1976, **98**, 2134; (b) Davies, J. A., Hartley, F. R. and Murray, S. G., *Inorg. Chem.*, 1980, **19**, 2299; (c) Sen, A. and Lai, T. W., *Organometallics*, 1982, **1**, 415.
 - Boéré, R. T., Montgomery, C. D., Payne, N. C. and Willis, C. J., *Inorg. Chem.*, 1985, **24**, 3680.
 - (a) Blake, A. J., Gould, R. O., Lavery, A. J. and Schröder, M., *Angew. Chem. Int. Ed. Engl.*, 1986, **25**, 274; (b) Wiegardt, K., Küppers, H.-J., Raabe, E. and Krüger, C., *Angew. Chem. Int. Ed. Engl.*, 1986, **25**, 1101; (c) Blake, A. J., Holder, A. J., Hyde, T. I., Roberts, Y. V., Lavery, A. J. and Schröder, M., *J. Organomet. Chem.*, 1987, **323**, 261; (d) Grant, G. T., Sanders, K. A., Setzer, W. N. and VanDerveer, D. G., *Inorg. Chem.*, 1991, **30**, 4053; (e) de Groot, B., Hanan, G. S. and Loeb, S. J., *Inorg. Chem.*, 1991, **30**, 4644.
 - Blake, A. J., Crofts, R. D., de Groot, B. and Schröder, M., *J. Chem. Soc., Dalton Trans.*, 1993, 485.
 - (a) Protopopov, I. S. and Kraft, M. Ya., *Zh. Obshch. Khim.*, 1963, **33**, 3050; (b) Protopopov, I. S. and Kraft, M. Ya., *Med. Prom. USSR*, 1959, **13**, 5.
 - (a) Thomas, R. R. and Sen, A., *Inorg. Synth.*, 1989, **26**, 128; (b) de Renzi, A., Panunzi, A. and Vitagliano, A., *J. Chem. Soc., Chem. Commun.*, 1976, 47; (c) Hendrickson, D. N., Sohn, Y. S. and Gray, H. B., *Inorg. Chem.*, 1971, **10**, 1559.
 - TEXSAN-TEXRAY Structure Analysis Package, Molecular Structure Corporation, 1985, 1996.
 - SHELXTL v. 5.04, G. M. Sheldrick and Siemens Analytical X-ray Systems, Inc., 1997, 6300 Enterprise Lane, Madison WI, 53719.
 - MITHRIL: Integrated Direct Methods Computer Program, Gilmore, C. J., *J. Appl. Cryst.*, 1984, **17**, 42.
 - DIRDIF: Direct Methods for Difference Structure, An Automatic Procedure for Phase Extension; Refinement of Difference Structure Factors: Beurskens, R. T. Technical Report, 1984.
 - PHASE: Calbrese, J. C., *PHASE—Patterson Heavy Atom Solution Extractor*. University of Wisconsin, Madison, PhD. Thesis, 1972.
 - (a) Wiegardt, K., Walz, W., Nuber, B., Weiss, J., Ozarowski, A., Stratemeier, H. and Reinen, D., *Inorg. Chem.*, 1986, **25**, 1650; (b) Zompa, L. J. and Margulis, T. N., *Inorg. Chem. Acta*, 1978, **28**, L157.
 - (a) Bosnich, B., Mason, R., Pauling, P. J., Robertson, G. B. and Tobe, M. L., *J. Chem. Soc., Chem. Commun.*, 1968, 97; (b) Ito, T., Sugimoto, M., Toriumi, K. and Ito, H., *Chem. Lett.*, 1981, 1477; (c) van der Merwe, M. J., Boeyens, J. C. A. and Hancock, R. D., *Inorg. Chem.*, 1983, **22**, 3489; (d) Wada, A., Sakabe, N. and Tanaka, J., *Acta Crystallogr.*, 1976, **B32**, 1121; (e) Szalda, D. J., Macartney, D. H. and Sutin, N., *Inorg. Chem.*, 1984, **23**, 3473; (f) Krüger, H.-J. and Holm, R. H., *J. Am. Chem. Soc.*, 1990, **112**, 2955.
 - (a) Holm, R. H. and Krüger, H.-J., *Inorg. Chem.*, 1987, **26**, 3647; (b) Castro, B. and Freire, C., *Inorg. Chem.*, 1990, **29**, 5113; (c) Choudhury, S. B., Ray, D. and Chakravorty, A., *Inorg. Chem.*, 1990, **29**, 4603; (d) Krüger, H.-J., Peng, G. and Holm, R. H., *Inorg. Chem.*, 1991, **30**, 734; (e) Franolic, J. D., Wang, W. Y. and Millar, M., *J. Am. Chem. Soc.*, 1992, **114**, 6587 and references therein; (f) Blake, A. J., Gould, R. O., Halcrow, M. A., Holder, A. J., Hyde, T. I. and Schröder, J. *Chem. Soc., Chem. Commun.*, 1992, 3427; (g) Cha, M., Gatlin, C. L., Critchlow, S. C. and Kovacs, J. A., *Inorg. Chem.*, 1993, **32**, 5868.
 - (a) Armstrong, J. McD., Meyer, D. V., Verpoorte, J. A. and Edsall, J. T., *J. Biol. Chem.*, 1966, **241**, 5137; (b) Chlebowski, F. and Coleman, J. E., *Metal Ions in Biological Chemistry*, ed. H. Sigel, 1976, **6**, 1.
 - (a) *Comprehensive Coordination Chemistry*, Vol. 5, ed. G. Wilkinson, R. D. Gillard, and J. A. McCleverty, Pergamon Press, Oxford, U.K., 1987, chap. 52 and references therein.
 - (a) Garrou, P. E., *Chem. Rev.*, 1981, **81**, 229; (b) Lindner, E., Hausteim, M., Mayer, H. A., Schneller, T., Fawzi, R. and Steinmann, E., *Inorg. Chim. Acta*, 1995, **231**, 201.
 - (a) Alcock, N. W., Platt, A. W. and Pringle, P., *J. Chem. Soc., Dalton Trans.*, 1987, 2273; (b) Alcock, N. W., Platt, A. W. G. and Pringle, P. G., *J. Chem. Soc., Dalton Trans.*, 1989, 139.